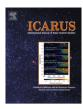


Contents lists available at SciVerse ScienceDirect

## **Icarus**

journal homepage: www.elsevier.com/locate/icarus



# Saturn's thermal emission at 2.2-cm wavelength as imaged by the Cassini RADAR radiometer



M.A. Janssen <sup>a,\*</sup>, A.P. Ingersoll <sup>b</sup>, M.D. Allison <sup>c</sup>, S. Gulkis <sup>a</sup>, A.L. Laraia <sup>b</sup>, K.H. Baines <sup>a</sup>, S.G. Edgington <sup>a</sup>, Y.Z. Anderson <sup>a</sup>, K. Kelleher <sup>a</sup>, F.A. Oyafuso <sup>a</sup>

- <sup>a</sup> Jet Propulsion Laboratory, California Institute of Technology, Pasadena, CA, 91109, United States
- <sup>b</sup> California Institute of Technology, Pasadena, CA, 91125, United States
- <sup>c</sup> NASA Goddard Institute for Space Studies, New York, NY, 10025, United States

#### ARTICLE INFO

Article history: Available online 21 June 2013

Keywords: Saturn, Atmosphere Atmospheres, Structure Atmospheres, Composition Radiative transfer Radio observations

#### ABSTRACT

We present well-calibrated, high-resolution maps of Saturn's thermal emission at 2.2-cm wavelength obtained by the Cassini RADAR radiometer through the Prime and Equinox Cassini missions, a period covering approximately 6 years. The absolute brightness temperature calibration of 2% achieved is more than twice better than for all previous microwave observations reported for Saturn, and the spatial resolution and sensitivity achieved each represent nearly an order of magnitude improvement. The brightness temperature of Saturn in the microwave region depends on the distribution of ammonia, which our radiative transfer modeling shows is the only significant source of absorption in Saturn's atmosphere at 2.2-cm wavelength. At this wavelength the thermal emission comes from just below and within the ammonia cloud-forming region, and yields information about atmospheric circulations and ammonia cloud-forming processes. The maps are presented as residuals compared to a fully saturated model atmosphere in hydrostatic equilibrium. Bright regions in these maps are readily interpreted as due to depletion of ammonia vapor in, and, for very bright regions, below the ammonia saturation region. Features seen include the following: a narrow equatorial band near full saturation surrounded by bands out to about 10° planetographic latitude that demonstrate highly variable ammonia depletion in longitude; narrow bands of depletion at -35° latitude; occasional large oval features with depleted ammonia around  $-45^{\circ}$  latitude; and the 2010–2011 storm, with extensive saturated and depleted areas as it stretched halfway around the planet in the northern hemisphere. Comparison of the maps over time indicates a high degree of stability outside a few latitudes that contain active regions.

© 2013 Elsevier Inc. All rights reserved.

### 1. Introduction

The thermal emission from the gas giant planets was first observed by single-antenna telescopes in the 1950s (Mayer et al., 1958), and quantitatively related to fundamental atmospheric properties in the following decade (Thornton and Welch, 1963; Gulkis et al., 1969; Wrixon and Welch, 1970). Subsequent observations through the 1980s filled in the disk-temperature spectra of Jupiter and Saturn through the millimeter- and centimeter-wavelength range. This combined with advances in understanding the high-pressure microwave absorption of ammonia, which possesses a strong inversion band just longward of 1-cm wavelength, led to a consistent story of deeply convective atmospheres with ammonia as the dominant absorber (Gulkis and Poynter, 1972; Berge and Gulkis, 1976; Klein and Gulkis, 1978). The whole disk spectrum through the microwave region for Saturn led to a value for the deep

atmosphere mixing ratio of ammonia of about three times the solar abundance, value consistent with previous work (de Pater, 1990; Atreya, 2010), and our analysis in L13. The measured disk temperature spectrum of Saturn may be found in de Pater and Massie (1985) and van der Tak et al. (1999).

The advent around the same time of radio interferometers capable of using aperture synthesis to image the planets led to the first microwave image of Saturn, reported by Schloerb et al. (1979) using the interferometer Owens Valley Radio Observatory at 3.7-cm wavelength. The completion of the National Radio Astronomical Observatory's Very Large Array in New Mexico was followed by a series of images of Saturn and its rings made with this instrument reported by a number of authors at wavelengths ranging from 2- to 21-cm wavelength (e.g., de Pater and Dickel, 1982, 1991; Grossman et al., 1989; Grossman, 1990). These studies have resulted in a better understanding of Saturn's rings and atmospheric microwave spectrum, and have provided evidence of large-scale structure in Saturn's ammonia distribution including variable broad bands in the midlatitudes. However, they have been

<sup>\*</sup> Corresponding author. Fax: +1 818 354 8895. E-mail address: michael.a.janssen@jpl.nasa.gov (M.A. Janssen).

**Table 1**Nominal radiometer characteristics.

Frequency	13.78 GHz
Wavelength	2.18 cm
Polarization	One linear
Radiometer bandpass	135 MHz
Measurement noise	0.026 K/√Hz
Beam full width	0.36° Circular
at half-power (beam 3)	

limited by the capabilities of the VLA in spatial resolution and dynamic range for imaging extended objects, in addition to which the process of Earth-rotational aperture synthesis used for imaging averages out longitudinal structure. The theoretical capability for the synthesized beam of the VLA in its largest (D) configuration is 1.3" at 2-cm wavelength, providing spatial resolution on Saturn comparable to that achieved here (1° latitude at the equator). However, results published to date show actual spatial resolutions achieved to be 6° or greater in latitude (e.g., Grossman et al., 1989; van der Tak et al., 1999; Dunn et al., 2002).

The presence of a microwave radiometer in orbit around Saturn provides a unique opportunity to image Saturn with the advantage of close range and without the limitations of a ground-based approach. In this paper we present global maps of Saturn obtained over the course of the Cassini prime and equinox missions by the radiometer that is incorporated into the Cassini RADAR instrument. The emphasis in this paper is to describe the observations, the mapping approach, and overall interpretations. We describe the observational approach and calibration in the next section. In Section 3 we concentrate on the generation of the maps and their interpretation in terms of the ammonia distribution, followed by a discussion of the nature and magnitude of residual errors in the maps. We pay particular attention to the latter since the mapping approach is unique. In Section 4 we offer a discussion and general interpretation of the features seen in the maps, leaving a more detailed discussion of the broader implications to a companion paper by Laraia et al. (2013), henceforth referred to as L13.

#### 2. Observations

# 2.1. The Cassini radiometer

The Cassini RADAR instrument includes a radiometer that obtains measurements of externally generated (passive) radiation entering the receiver in all operating modes of the instrument, including the various radar modes during which internally-generated (active, or radar) signals are transmitted (Elachi et al., 2004; West et al., 2009; Janssen et al., 2009). The overall characteristics of the radiometer are given in Table 1. The RADAR instrument operates in repetitive "burst" cycles, in which each cycle is divided into active (radar transmit/receive) and passive (radiometer) segments. The radiometer segment employs a Dicke-switching technique in which the noise power received through the antenna is

compared with that from an internal reference blackbody termination using a microwave switch to select either the external (sky) signal or an internal reference, using the comparison to stabilize the sky signal. In general operation a second switch is used to select among an array of five antenna feeds; e.g., cycling through these enable synthetic aperture radar observations to be obtained in a wide swath. The duration of the transmit/receive period is adjustable, as are the number and duration of the radiometer averaging intervals. In the Saturn observations we used a 1-s duration burst cycle in which the active segment was eliminated and the antenna was set to the central (and smallest) radar beam, beam 3. The radiometric segment was expanded to observe the target for the entire 1-s period except for a 25 ms integration on the reference load in each cycle, These choices provided the beamwidth and sensitivity given in Table 1.

#### 2.2. Observational approach

The RADAR radiometer was used to observe Saturn during five equatorial periapsis passes occurring between 2005 and 2011 for the purpose of mapping its 2.2-cm thermal emission. The dates and general orbital parameters for these observations are given in Table 2, and details helpful for the interpretation of the maps are given in Table 3. The observations were centered approximately on the periapsis of each pass in order to obtain the best achievable spatial resolution, which is important given that the 0.36° beamwidth of the radiometer is large compared to the resolutions of typical imaging instruments. Saturn presents a challenge comparable to that of Titan for mapping and calibration – it is an extended source that requires a large number of individual observations to build an image, each of which must be corrected for gain and baseline drift as well as signal contamination by sidelobe contributions. The approach developed for Titan for calibration and sidelobe contribution removal was carried over directly to Saturn and is described further below. The actual mapping strategy was necessarily different than the raster scanning and long-term mosaicking approach used on Titan, however, because of the different spacecraft trajectories relative to the target and Saturn's rapidly changing surface structure. Our approach for Saturn was to scan repetitively from pole to pole through Saturn's nadir as rapidly as practical as the spacecraft moved along its trajectory through periapsis, letting the motion of the spacecraft combined with Saturn's rotation provide the westward longitudinal component of the scan. Each scan took from five to ten minutes depending on range, during which time the subspacecraft longitude increased somewhat more than a beamwidth. This led to a spatial asymmetry in sampling discussed further below. Fig. 1 shows both the scan pattern of the beam axis in inertial space as it progressed with time, and as a track on the surface of Saturn, where we take the December 2009 pass as an example (the underlying map is derived from the data as described later in this paper). The gap at approximately 11 h (25° west longitude in the lower panel) was caused by the need to unload the spacecraft momentum wheels. In the lower

**Table 2** Mapping orbit characteristics.

Date	Start time (UT)	Segments	Mapping duration (h)	S/C orbit inclination relative to Saturn (°)	Ring plane crossing longitude (°W Lon.)	Periapsis	
						Distance $(R_S)$	Saturn longitude (°W Lon.)
September 23, 2005	2005 SEP 23 11:15	3	22.78	0.32	_	2.002	298.3
October 13, 2009	2009 OCT 13 23:26	4	11.83	0.55	190.5	2.198	148.5
December 09, 2009	2009 DEC 09 22:58	2	13.94	0.50	18.1	2.220	313.9
July 24, 2010	2010 JUL 24 22:15	2	12.90	4.66	282.1	2.475	312.7
March 20, 2011	2011 MAR 20 04:03	1	14.08	0.38	_	3.722	257.8

# Download English Version:

# https://daneshyari.com/en/article/10701321

Download Persian Version:

https://daneshyari.com/article/10701321

<u>Daneshyari.com</u>